Modeling of Nonlinear Control with Disturbance Observer-Based Parameter Estimation for Permanent Magnet Synchonous Motor

*S. Sriprang[1,2,3], B. Nahid-Mobarakeh[1], S. Pierfederici[1], N. Takorabet[1], N. Bizon[5], P. Kumam[4] and P. Thounthong[2,3]

[1]GREEN Lab., Universite de Lorraine, 2 Vancouver-Ies-Nancy, Lorraine 54516, France
[2]Renewable Energy Research Centre (RERC), Thai-French Innovation Institute (TFII)
[3]Department of Teacher Training in Electrical Engineering (TE), Faculty of Technical Education
King Mongkut's University of Technology North Bangkok, 1518, Pracharat 1 Rd., Bangkok 10800, Thailand
*e-mail: songklod.sri@rmutr.ac.th
[4]Department of Mathematics, King Mongkut's University of Technology Thonburi, Bangkok, Thailand
[5]Faculty of Electronics, Communications and Computers, University of Pitesti, Arges 110040, Pitesti, Romania

***Abstract*— This paper presents a new parametric system identification method for estimating the parameters of PMSM consisting of the inductance series resistance of motor wiring and switching losses of semiconductors represented by v_{tq} as well as load torque disturbance T_L based on Disturbance Observer (DOB) and the nonlinear based control modeling for controlling PMSM. The proposed average models include parameter modeling the losses and their estimation. The hardware system of the PMSM control is implemented by using a small-scale PMSM of 6-pole, 1-kW, and 3000 rpm in a laboratory, to validate the proposed methodology. Simulation and experimental validation show that a new state observer is better than the extended Luenberger observer (ELO) method towards convergence for nonlinear systems and convergence rapidity.**

***Keywords*— Disturbance observer (DOB); SPMSM; Flatness-based control modeling; Extended Luenberger Observer (ELO);**

I. INTRODUCTION

Despite its advantages, it is still challenging to control the PMSM to achieve good transient performance under all operating conditions. This is due to the fact that the PMSM is a nonlinear multivariable time-varying system and subjected to unknown disturbance. Therefore, nonlinear control systems are more suitable for controlling permanent magnetic synchronous motors than for linear systems [2]. One of the nonlinear control systems that are used to control the permanent magnet synchronous motors is the flatness control system [3]. However, flatness control is based on the system model. So its performance largely depends on the accuracy of model parameters such as the stator resistance R_s, load torque T_L, etc. The new parameter estimation methods are proposed in this paper to address this problem. And also, the comparison between a new parameter estimation method and extended Luenberger observer method is going to considered emphasizing the interest of the proposed parameter estimation concerning convergence for nonlinear systems and convergence rapidity.

II. DESING OF THE ROBUST FLATNESS CONTROL

A. Mathematics Model of the PMSM/inverter

Figure 1 shows the inverter system used to control PMSM in this research. The classic rotor reference frame equations of the PMSM are

$$\frac{di_d}{dt} = \frac{1}{L_d}(v_d - R_s \cdot i_d + \omega_e \cdot L_q \cdot i_q) \quad (1)$$

$$\frac{di_q}{dt} = \frac{1}{L_q}(v_q - R_s \cdot i_q - \omega_e \cdot L_d \cdot i_d - \omega_e \cdot \Psi_m) \quad (2)$$

$$\frac{d\omega_m}{dt} = \frac{1}{J}(T_e - B_f \cdot \omega_m - T_L) \quad (3)$$

where

$$T_e = p \cdot i_q \cdot (\Psi_m - (L_q - L_d) \cdot i_d) \quad (4)$$

$$\omega_e = p \cdot \omega_m \quad (5)$$

v_d, v_q are the d, q-axis voltages, i_d, i_q are the d, q-axis stator currents, L_d and L_q are the d, q-axis inductances, R_s and ψ_m are the resistance and flux linkage, respectively; and ω_e, ω_m, p, T_e, T_L, B_f, J are electrical angular frequency, mechanical angular frequency, number of pole pairs, electromagnetic torque, load torque, viscosity, and inertia, respectively.

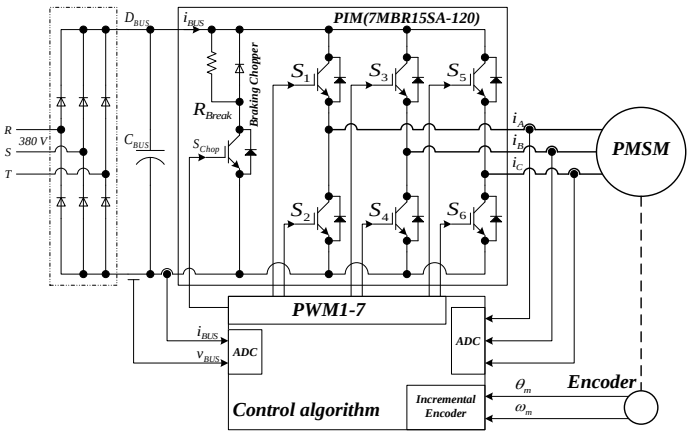

Fig. 1. A three-phase inverter is driving the PMSM where v_{BUS}, i_{BUS}, i_A, i_B, i_C are DC bus voltage, the input inverter current, the motor phase current, respectively.

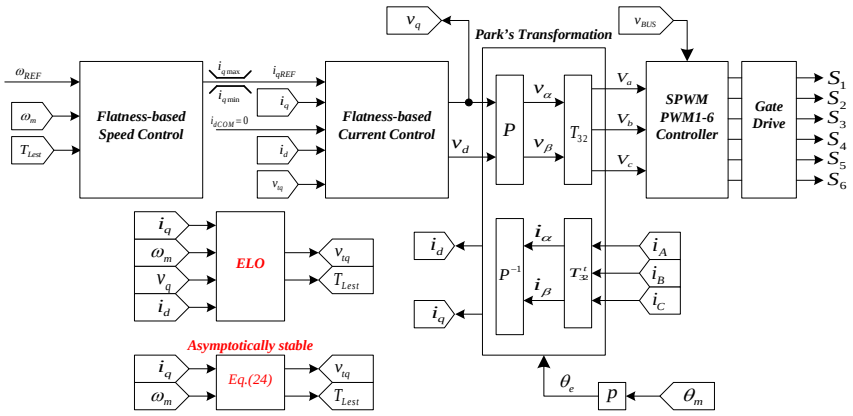

Fig. 2. Structure of the PMSM drive system with the flatness-based control and ELO.

B. *Flatness control design*

Figure 2 shows the whole control system of the PMSM control using the flat control system proposed in this research. For the first is to analyze the flatness-based control that is mentioned by [4], to utilize for PMSM control. As $L_s = L_q = L_d$ is defined for non-salient machine. Flat outputs $y = [i_d\ i_q\ \omega_m]^T$, control variable $u = [v_d\ v_q\ i_q]^T$, and state variable $x = [i_d\ i_q\ \omega_m]^T$ are assigned respectively. Then, the state variables x can be written as $x = [\varphi_1(y_1)\ \varphi_2(y_2)\ \varphi_3(y_3)]^T$. From (1), (2), and (3), the control variable u can be calculated from the flatness output y and its time derivatives (*called inverse dynamics*):

$$u_1 = L_s \cdot \dot{i}_d + R_s \cdot i_d - \omega_e \cdot L_s \cdot i_q = \psi_1(y_1, \dot{y}_1, y_2) = v_d \quad (6)$$

$$u_2 = L_s \cdot \dot{i}_q + R_s \cdot i_q + \omega_e \cdot L_s \cdot i_d + \omega_e \cdot \Psi_m = \psi_2(y_1, y_2, \dot{y}_2) = v_q \quad (7)$$

$$u_3 = (J \cdot \dot{\omega}_m + T_L + B_f \cdot \omega_m) / p \cdot \Psi_m = \psi_3(y_3, \dot{y}_3) = i_{qCOM} \quad (8)$$

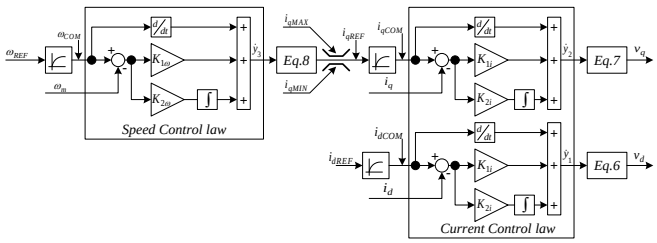

Fig. 3. Proposed flatness-based control with state observer for PMSM drive.

The control law of the current and speed control loop detailed depicts in Fig. 3. The input reference of each module of the current control is y_{iREF}, where i = 1, 2, ($y_{1REF} = i_d = 0$, and $y_{2REF} = i_{qCOM}$), and the input reference of the speed control is $y_{3REF} = \omega_{COM}$. The control law based on the second-order control law is used by (9) for current loop and (10) for the speed loop, to guarantee that the control of the flatness output variable converges to their reference trajectory.

$$\dot{y}_i = \dot{y}_{iREF} + K_{1i}(y_{iREF} - y_i) + K_{2i}\int_0^t (y_{iREF} - y_i)d\tau \quad (9)$$

$$\dot{y}_3 = \dot{y}_{3REF} + K_{1\omega}(y_{3REF} - y_3) + K_{2\omega}\int_0^t (y_{3REF} - y_3)d\tau \quad (10)$$

where K_{1i}, K_{2i}, $K_{1\omega}$, and $K_{2\omega}$ are the controller parameters defining as follows:

$$K_{1i} = 2\zeta_1\omega_1,\ K_{2i} = \omega_1^2,\ K_{1\omega} = 2\zeta_3\omega_3,\ K_{2\omega} = \omega_3^2$$

The tracking error ($e_1 = y_{iREF} - y_i$) and ($e_2 = y_{3REF} - y_3$) are defined that is

$$q_i(s) = e_1^2 + 2\zeta_1\omega_1 e_1 + \omega_1^2 \quad (11)$$

$$q_\omega(s) = e_2^2 + 2\zeta_3\omega_3 e_2 + \omega_3^2 \quad (12)$$

ζ_1 and ζ_3, are the desired dominant damping ratio, and ω_1 and ω_3 are natural frequency respectively.

It is evident that the control system is stable for the positive value of K_{1i}, K_{2i}, $K_{1\omega}$, and $K_{2\omega}$. However, "*based on a cascade control structure and constant switching frequency in power electronic inverters, the frequencies of the system must meet the following rule: $\omega_3 << \omega_1 << \omega_s$, where ω_3 is the cut off frequency of the speed control loop, ω_1 is the cut off frequency of the current control loop and ω_s is the switching frequency*" [2]. Finally, a second-order is used by (13) to limit the transient current and speed command, so that they are going to keep smooth transition during the instantaneous variation that is

$$\frac{\omega_{REF}(s)}{\omega_{COM}(s)} = \frac{i_{qREF}(s)}{i_{qCOM}(s)} = \frac{i_{dREF}(s)}{i_{dCOM}(s)} = \frac{1}{\left(\frac{s}{\omega_{ni}}\right)^2 + \frac{2\zeta_i}{\omega_{ni}}s + 1} \quad (13)$$

ζ_i and ω_{ni} where i = 2, 4 are the desired dominant damping ratio and natural frequency respectively

III. State Observer for Parameter Estimation

In this section discusses the implementation of the two state observer methods, including ELO and asymptotically stable respectively. Refer to the inverse dynamics equations (6), (7), and (8), the stator resistance R_s and external disturbance torque T_L are estimated by observer methods that are proposed to compare and investigate the best performance for estimating parameters. However, v_{tq} (=$R_s.i_q$) is defined in place of R_s.

To simplify the implementation and PMSM working in only constant torque region (i_d=0), (2) and (3) are rewritten that is:

$$\frac{di_q}{dt} = \frac{1}{L_q}(v_q - v_{tq} - \omega_e \cdot L_s \cdot i_d - \omega_e \cdot \Psi_m) \quad (14)$$

$$\frac{d\omega_m}{dt} = \frac{1}{J}(p \cdot \Psi_m \cdot i_q - B_f \cdot \omega_m - T_L) \quad (15)$$

A. Extended Luenberger Observer

The state observer equation by using the Luenberger observer is defined as follows [5].

$$\dot{\hat{x}}(t) = \mathbf{A}\hat{x}(t) + \mathbf{B}u(t) + \mathbf{L}(y(t) - \hat{y}(t)) \quad (16)$$

$$\hat{y}(t) = \mathbf{C}\hat{x}(t) \quad (17)$$

$$\dot{\hat{x}}(t) = \mathbf{A}\hat{x}(t) + \mathbf{B}u(t) + \mathbf{LC}(\hat{x}(t) - x(t)) \quad (18)$$

where $x(t) = [i_q\ \omega_m\ v_{tq}\ T_L]^T$, $y = [i_q\ \omega_m]^T$, and $u = [v_q\ i_d]$.

$$\mathbf{A} = \begin{bmatrix} 0 & -\frac{\Psi_m}{L_s} & -\frac{1}{L_s} & 0 \\ -\frac{p \cdot \Psi_m}{J} & -\frac{B_f}{J} & 0 & -\frac{1}{J} \\ 0 & 0 & 0 & 0 \\ 0 & 0 & 0 & 0 \end{bmatrix} \mathbf{B} = \begin{bmatrix} \frac{1}{L_s} & -p \cdot \omega_{m0} \\ 0 & 0 \\ 0 & 0 \\ 0 & 0 \end{bmatrix}$$

$$\mathbf{C} = \begin{bmatrix} 1 & 0 & 0 & 0 \\ 0 & 1 & 0 & 0 \end{bmatrix} \quad (19)$$

If the observer gain **L** making the matrix (**A**-**LC**) to be stable is suitably designed, the estimation will converge, and the estimated error $e(t) = \hat{x}(t) - x(t)$ tends to zero. By using Ackermann's formula [3] and choosing (**A**-**LC**) eigenvalues approach $(-10000\ -10000\ -18\ -30)^T$, the observer gain matrix **L** can be appropriately determined as shown by (20), at speed (n) = 1500 rpm ω_{m0} = 157.0796 rad/sec, and $i_{d(0)} = 0$.

$$\mathbf{L} = \begin{bmatrix} 260 & -18.811 \\ 395.357 & 230.9174 \\ -423.720 & 0 \\ 0 & -11.088 \end{bmatrix} \quad (20)$$

For this estimation, even if the system has already linearized around one operating point, it has been experimentally verified that this one was converging in the speed range 0-1500 rpm with no change of the value of the matrix **L**.

B. New State Observer Design

In this section introduces a new state observer. The proposed state observers are devoted to the subclass of nonlinear systems, which can describe as follows [6]:

$$\begin{cases} \dot{\mathbf{X}} = \begin{pmatrix} \dot{x} \\ \dot{d} \end{pmatrix} = \begin{pmatrix} f(x,u) + g(x,u) \cdot d \\ 0 \end{pmatrix} \\ \mathbf{Y} = x \end{cases} \quad (21)$$

where:

1) $\dot{\mathbf{X}} \in \mathbb{R}^{n*m}$ is the vector of the variable which is going to be estimated, and $\mathbf{Y} \in \mathbb{R}^n$ is the vector of measured variable;

2) $x \in \mathbb{R}^n$ is the vector of the system state variable. Every state variable is supposed to be measured (i.e., $\mathbf{Y} = x$);

3) $d \in \mathbb{R}^m$ is the vector of unknown parameters to estimate. Variable d is supposed to very slowly compared to state variables x;

4) f and g are nonlinear functions of x and u (the command signal vector), respectively, of size $\mathbb{R}^n$ and $\mathbb{R}^{n*m}$

Refer to (14) and (15), the first is to define state variable x, unknown parameters d, f, and g, respectively that is $x = [i_q\ \omega_m]^T$ and $d = [v_{tq}\ T_L]^T$.

$$f(x,u) = \begin{bmatrix} \frac{1}{L_s}\left(v_q - \omega_e \cdot L_s \cdot i_d - \omega_e \cdot \Psi_m\right) \\ \frac{1}{j}\left(p \cdot \Psi_m \cdot i_q - B_f \cdot \omega_m\right) \end{bmatrix} \quad (22)$$

$$g(x,u) = \begin{bmatrix} \frac{-1}{L_s} & 0 \\ 0 & \frac{-1}{J} \end{bmatrix} \quad (23)$$

Asymptotically stable

For the subclass of nonlinear systems verifying (21), the proposed state observer is defined through (24), considering the estimation error $e_x = (\hat{x} - x)$ and $e_x = (\hat{d} - d)$

$$\begin{pmatrix} \dot{\hat{x}} \\ \dot{\hat{d}} \end{pmatrix} = \begin{bmatrix} f(x,u) + g(x,u) \cdot \hat{d} - \mathbf{S}_1 \cdot e_x \\ -g^T(x,u) \cdot e_x \end{bmatrix} \quad (24)$$

with

$\mathbf{S}_1$ is the positive-definite matrix of size $\mathbb{R}^{n*m}$.

Proof: the derivative estimation error e_x and e_d are written by (25), (26)

$$\dot{e}_x = g(x,u) \cdot e_d - \mathbf{S}_1 \cdot e_x \quad (25)$$

$$\dot{e}_d = -g^T(x,u) \cdot e_x \quad (26)$$

Asymptotic stability of the estimation can demonstrate with the classical Lyapunov approach. For this the Lyapunov candidate function, $\boldsymbol{V}$ is considered as follows:

$$V = \frac{1}{2}\begin{pmatrix} e_x & e_d \end{pmatrix} \cdot \begin{pmatrix} e_x \\ e_d \end{pmatrix} \geq 0 \quad (27)$$

The derivative of function $\boldsymbol{V}$ can express as

$$\dot{V} = e_x^T \cdot \dot{e}_x + e_d^T \cdot \dot{e}_d \quad (28)$$

By combining (25), (26), and (28), $\dot{\boldsymbol{V}}$ can be expressed as

$$\dot{V} = e_x^T \cdot g(x,u) \cdot e_d - e_x^T \cdot \mathbf{S}_1 \cdot e_x + e_d^T(-g(x,u) \cdot e_x) \quad (29)$$

Finally,

$$\dot{V} = -e_x^T \cdot \mathbf{S}_1 \cdot e_x < 0 \quad (30)$$

From (27) and (30), the asymptotic estimation stability [4] can guarantee as long as $\mathbf{S}_1$ is the positive-definite matrix.

IV. Simulation and Experimental Validate

A. Laboratory setup

The main PMSM parameters are defined by Table 1, and the flatness controller parameters are determined by Table 2. The laboratory setup shows in Fig. 4. composed of a 6-pole, 1-kW PMSM coupled with a 0.25-kW Separate Excited DC motor served as a power supply for a purely resistive load.

TABLE I.

Symbol.	PMSM/Inverter specification and parameters	
	Meaning	*Value*
P_{rated}	Rated Power	1 kW
n_{rated}	Rated Speed	3000 rpm
T_{rated}	Torque Rated	3 Nm
p	Number of Poles pair	3
R_s	Resistance (Motor + Inverter)	10.1 Ω
$L=L_d=L_q$	Stator inductance	35.31 mH
Ψ_m	Magnetic flux	0.2214 Wb
J	Equivalent inertia	0.0022 kg.m^2
B	Viscous friction coefficient	3.5 x 10^{-3} Nm.s/rad
f_s	Switching frequency	10 x 10^3 Hz

TABLE II.

Symbol.	Speed/current regulation parameters	
	Meaning	*Value*
ζ_1	Damping ratio 1	1 pu.
ω_{n1}	Natural frequency 1	3200 Rad.s^{-1}
ζ_2	Damping ratio 2	1 pu.
ω_{n2}	Natural frequency 2	320 Rad.s^{-1}
ζ_3	Damping ratio 3	1 pu.
ω_{n3}	Natural frequency 3	32 Rad.s^{-1}
ζ_4	Damping ratio 4	1 pu.
ω_{n4}	Natural frequency 4	32 Rad.s^{-1}
i_{qmax}	The max. quadrature current	+6 A
i_{qmin}	The min. quadrature current	-6 A

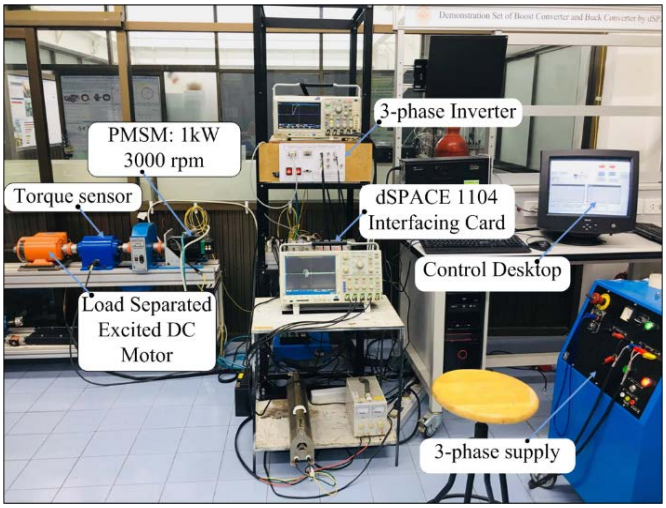

Fig. 4. Test laboratory setup of the PMSM drive.

The stator windings of the PMSM were fed by a 3 kW 3Φ dc–ac voltage-source inverter (VSI) operated at a switching frequency of 10 kHz. The input voltage is obtained through diode rectifier as shown in Fig. 1. The drive system was also equipped with an incremental encoder mounted on the rotor shaft and has a resolution of 4096 lines/revolution. The proposed controller was practically implemented using the dSPACE ds1104 board, with a time step of T_s = 1e-4.

B. Speed Reversal of flatness-based controller

The experimental results of speed reversal responses of the system are illustrated in Fig. 12, where the motor is forced to reverse its direction. The system operates in a regenerative mode until the speed of the rotor will become positive; and thereafter, the system changes to motoring mode until the rotor speed reaches reference value. The experimental results reflect that the speed of PMSM can efficiently be controlled by flatness control. During steady-state region, the speed measurement is able to almost 100% track the speed reference and the speed command, and *q*-axis current is restrained without exceeding the current limitation (+6 Ampere)

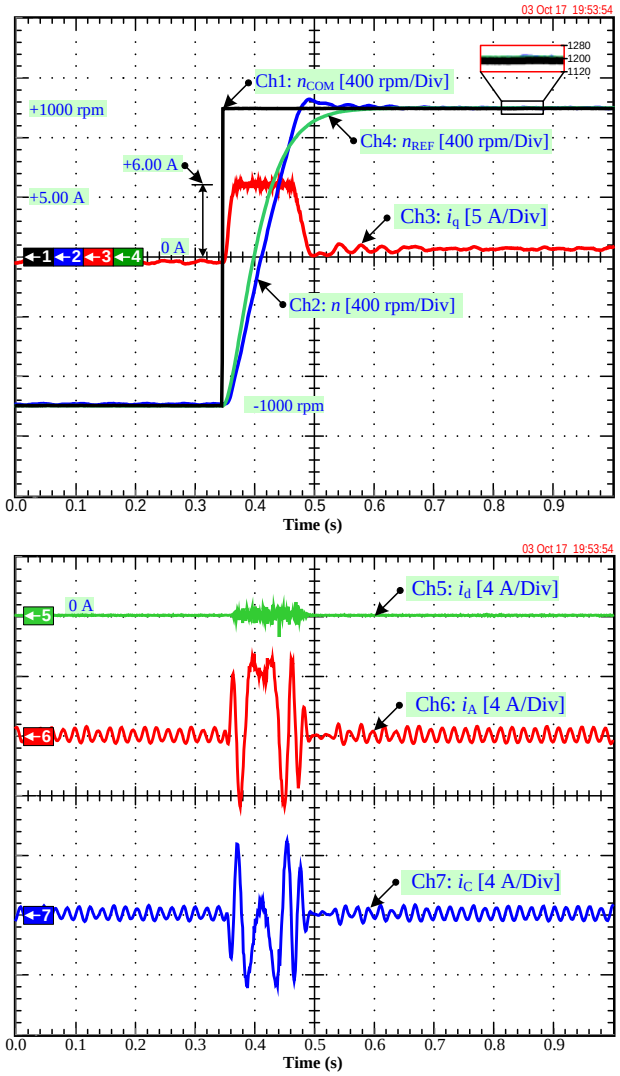

Fig. 5. Experimental results of speed reversal.

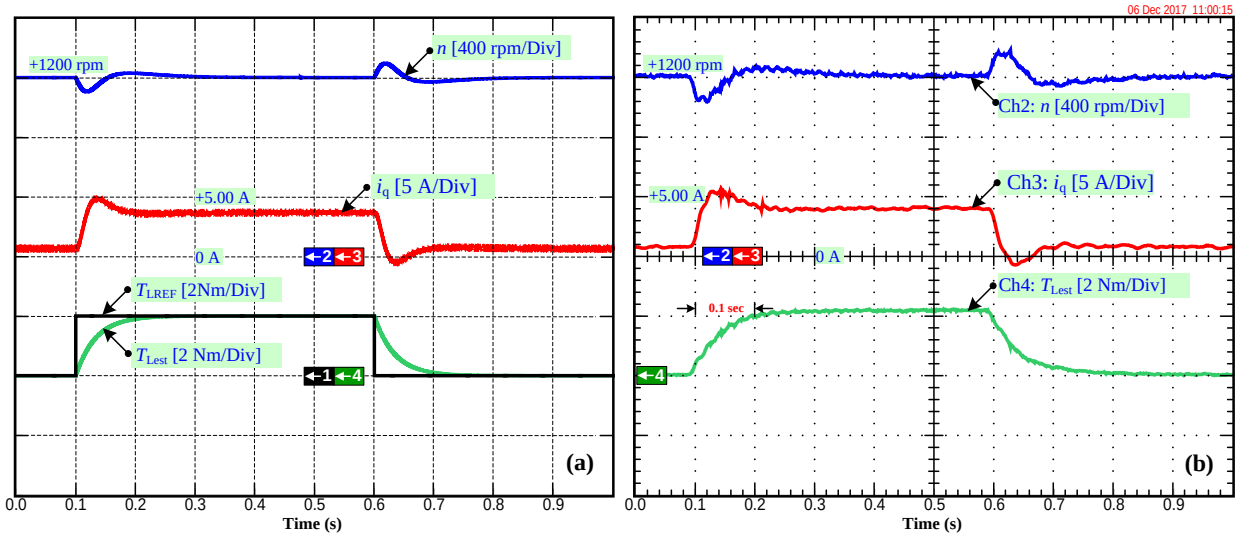

Fig. 6. Simulation and experimental results of TL estimation: (a) Simulation and (b) Experimental.

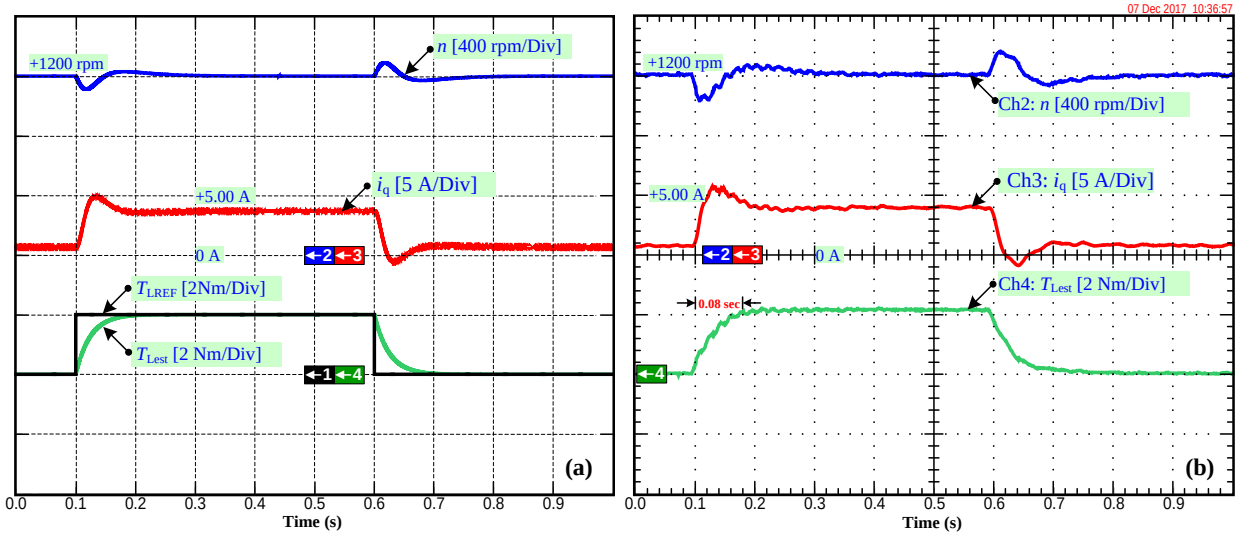

Fig. 7. Simulation and experimental results of TL estimation: (a) Simulation and (b) Experimental.

Next, Fig. 6(a) and 6(b) show the simulation and experimental results respectively of T_L estimation by using the asymptotically stable. The simulation and preliminary results indicate that both of them are coincident. The results reflect that when the external disturbance torque is suddenly taken from 0 Nm to 2 Nm, it can be correctly estimated by the asymptotically stable, and the converging time is less than 0.08 s that is slightly better than ELO. The results reflect that when the external disturbance torque is suddenly taken from 0 Nm to 2 Nm, it can be correctly estimated by the exponentially stable, and the converging time is less than 0.04 s that is distinctly better than ELO and the asymptotically stable

C. Performance of State Variables Estimation

Firstly, Fig. 5(a) and 5(b) show the simulation and experimental results respectively of T_L estimation by using ELO. The simulation and preliminary results indicate that both of them are coincident. The results reflect that when the external disturbance torque is suddenly taken from 0 Nm to 2 Nm, it can be correctly estimated by ELO, and the converging time is less than 0.1 s

D. Performance of disturbance rejection

In Fig. 8 to guarantee the stability of the control system, in this section is going to illustrate the response of the whole systems that including Ch1: v_{tq}, Ch2: speed measurement n, Ch3: q-axis current i_q, Ch4: T_{Lest}, Ch5: d-axis current i_d, Ch6: phase current i_a, Ch7: phase current i_c, and the trajectories of the transient stator current vector. The results reflect that the stability of flatness-based control and the exponentially stable is suitably designed. These results show that the exponentially stable has better disturbance rejection ability and result in the performance of the flatness-based control is improved because the performance of flatness-based control depends on these parameters of the system

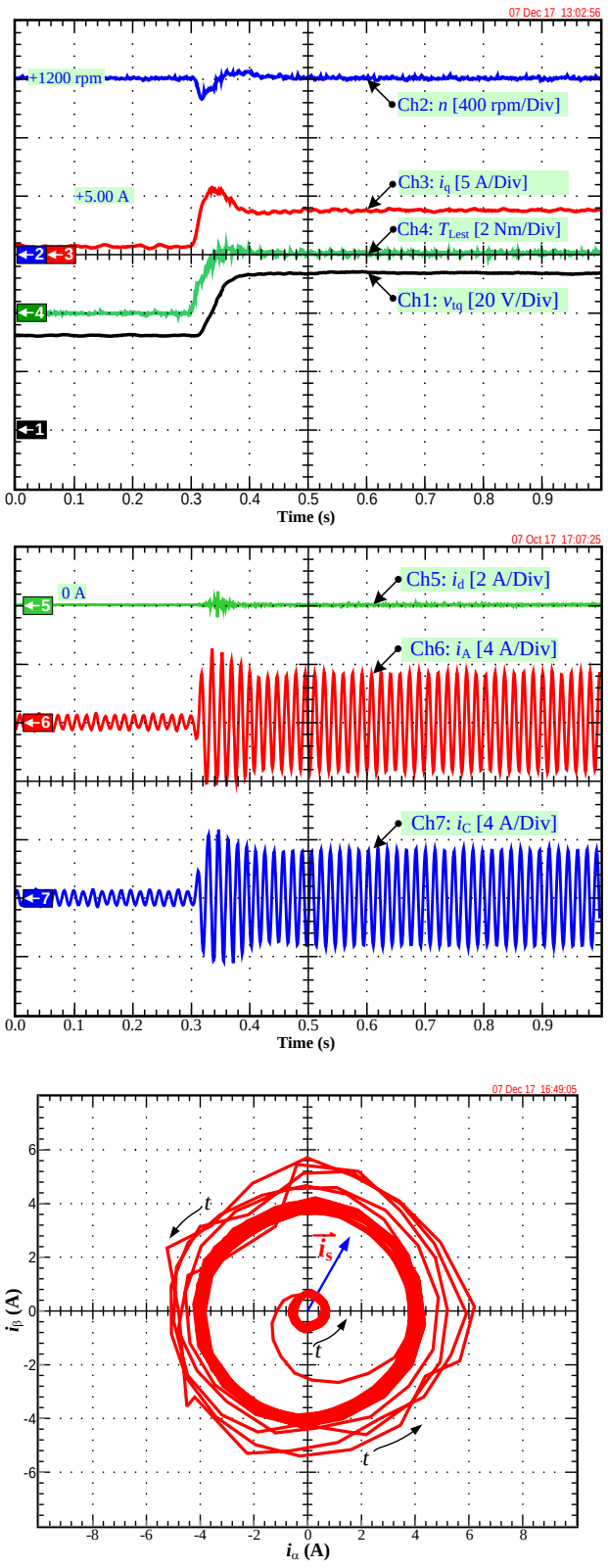

Fig. 8. Experimental results of disturbance rejection.

.

V. Conclusion

This paper has presented the state variables estimation using by using three state observer methods for the flatness-based control, including ELO, Asymptotically stable, and Exponentially stable to find and investigate the best performance for estimating parameters of PMSM consisted of T_L and v_{tq} of each the observer methods. Both the simulations and experiments show the interest of the exponentially stable methodology with better performances compared with ELO and an Asymptotically stable, especially for strongly nonlinear systems as shown in Fig.7(a) and 7(b). So within this paper, the exponentially stable was chosen to estimate parameters for flatness-based control. And also, the proposed modeling approach and the estimation by the proposed state observer can easily be adapted to other machine control. A laboratory setup was developed using a PMSM drive to practically illustrate the benefits of the proposed controller. The results have shown the ability of the proposed approach to reject the effect of the uncertainty disturbance torque that including parameters variation as shown in Fig.10. Thereby, the proposed control design provides practitioners with an alternative and effective method to build a robust flatness-based controller.

References

[1] B. Liu, B. Zhou and T. Ni and K. Hameyer, "Principle and Stability Analysis of an Improved Self-Sensing Control Strategy for Surface-Mounted PMSM Drives Using Second-Order Generalized Integrators," IEEE Trans. Energy Convers., vol. 33, no. 1, pp. 126-136, March 2018.

[2] H. Chaoui, M. Khayamy and O. Okoye, "Adaptive RBF Network Based Direct Voltage Control for Interior PMSM Based Vehicles," IEEE Trans. Vehicular Tech., vol. 67, no. 7, pp. 5740-5749, July 2018.

[3] P. Thounthong et al., “Model based control of permanent magnet AC servo motor drives,” in *Proc. Electrical Machines and Systems (ICEMS)*, 2016, pp. 1-6.

[4] P. Thounthong, A. Luksanasakul, P. Koseeyaporn, and B. Davat, “Intelligent model-based control of a standalone photovoltaic/fuel cell power plant with supercapacitor energy storage,” IEEE Trans. on Sustainable Energy, vol. 4, no. 1, pp. 240–249, Jan 2013.

[5] Dorf, R. C. and R. H. Bishop, “Modern control systems,” 12th ed., Pearson, 2011, pp. 847–850.

[6] H. Renaudineau, J. P. Martin, B. Nahid-Mobarakeh and S. Pierfederici, "DC–DC Converters Dynamic Modeling With State Observer-Based Parameter Estimation," *IEEE Trans. Power Electron.*, vol. 30, no. 6, pp. 3356-3363, June 2015.